An Unscented Kalman Filter Based Approach for the Health-Monitoring and Prognostics of a Polymer Electrolyte Membrane Fuel Cell

Xian Zhang[1], Pierluigi Pisu[2]

[1,2]*Department of Automotive Engineering, Clemson University, Clemson, SC, 29631, USA*

xianz@g.clemson.edu
pisup@clemson.edu

ABSTRACT

Poor long-term performance and durability combined with high production and maintenance costs remain the main obstacles for the commercialization of the polymer electrolyte membrane fuel cell (PEMFC). While on-line diagnosis and operating condition optimization play an important role in addressing the durability issue of the fuel cell, health-monitoring and prognosis (or PHM) techniques are of equally great significance in terms of scheduling condition-based maintenance (CBM) to minimize repair and maintenance costs, the associated operational disruptions, and also the risk of unscheduled downtime for the fuel cell systems.

In this paper, an unscented Kalman filter (UKF) approach is proposed for the purpose of damage tracking and remaining useful life (RUL) prediction of a PEMFC. To implement this model-based PHM framework, a physics-based, prognostic-oriented catalyst degradation model is developed to characterize the fuel cell damage that establishes the relationship between the operating conditions and the degradation rate of the electro-chemical surface area (ECSA). The model complexity is kept minimal for on-line prognostic purpose. Simulation is carried out for validation of the proposed algorithm, using a more detailed catalyst degradation model.

1. INTRODUCTION

To date long-term performance and durability of the fuel cells are difficult to quantify because not all degradation mechanisms of the various fuel cell components are completely understood. The fuel cell's performance degrades irreversibly throughout its lifetime mainly due to the following components' degradations: 1) catalyst degradation (catalyst particle coarsening); 2) carbon support degradation (carbon corrosion); and 3) membrane degradation (chemical deterioration and dehydration) (Okada, 2003; Schmittinger & Vahidi, 2008). Depending on the power load among other long-term operating conditions of the fuel cell, the extent of performance and durability degradation varies. General speaking, the longer the fuel cell stack is operated in transient or cycling conditions, or detrimental operating conditions such as flooding, the stronger is the corrosion and therefore the degradation. While on-line diagnosis and operating condition optimization play an important role in addressing the durability issue of the fuel cell, prognostics and health-monitoring (PHM) techniques are of equally great significance in terms of scheduling condition-based maintenance (CBM) to minimize repair and maintenance costs, the associated operational disruptions, and also the risk of unscheduled downtime for the fuel cell systems. However, so far little work has been done in the field of prognostics on fuel cell.

Bayesian based filtering techniques have found more and more use in the prognostic area due to their systematic and elegant treatment of the uncertainty management problem (Daigle, Saha, & Goebel, 2012; Saha & Goebel, 2008; Saha, Goebel, Poll, & Christophersen, 2007, 2009). Among these techniques, particle filtering (PF) has by far gained the most interest for its ability to handle arbitrary distributions and nonlinearities, and ease of implementation. Orchard et al. (M. E Orchard & Vachtsevanos, 2009; M. Orchard, Wu, & Vachtsevanos, 2005; Marcos E. Orchard & Vachtsevanos, 2007) proposed a novel particle filtering based prognostic framework. This approach employs a state dynamic model and a measurement model to predict the posterior probability density function of the state, that is, to predict the time evolution of a fault or fatigue damage. It avoids the linearity and Gaussian noise assumption of Kalman filtering and provides a robust framework for long-term prognosis while accounting effectively for uncertainties. Correction

terms are estimated in a learning paradigm to improve the accuracy and precision of the algorithm for long-term prediction. The approach is applied to a crack fault, and the results support its robustness and superiority.

Unscented Kalman filter (UKF), on the other hand, can also deal with nonlinearities in the system dynamics by approximating the state probability distribution with deterministic sigma points. While Gaussian distribution has to be assumed for the states and the noises, the UKF method brings great advantages of computational efficiency. In the case study provided in (Daigle et al., 2012), the UKF based prognostics approach outperforms that based on PF both in terms of computational cost and the accuracy measured by $\alpha-\lambda$ metrics, thus is considered to be a promising on-line prognostic tool.

This paper investigates the application of a UKF-based PHM scheme on the prognostics of a PEMFC. The paper is organized as follows: in Section 2, the UKF based framework for PHM is introduced; Section 3 presents a prognostic-oriented catalyst degradation model for the fuel cell; and in Section 4 we apply the UKF approach to the damage variable tracking and long term damage variable prediction of the fuel cell, as well as the RUL prediction and related performance metrics. The conclusion is presented finally in Section 5.

2. UKF-BASED FRAMEWORK FOR PHM

2.1. Bayesian Framework for Joint Estimation

We first consider a general joint estimation problem based on the following discrete system.

$$\begin{aligned}\mathbf{x}_{k+1} &= \mathbf{F}\left(\mathbf{x}_k, \mathbf{u}_k, \mathbf{v}_k, \mathbf{w}_k\right)\\ \mathbf{y}_k &= \mathbf{H}\left(\mathbf{x}_k, \mathbf{u}_k, \mathbf{n}_k, \mathbf{w}_k\right)\end{aligned} \tag{1}$$

where $\mathbf{x}_k$ represent the sates of the system, $\mathbf{y}_k$ the outputs, $\mathbf{u}_k$ the inputs , $\mathbf{v}_k, \mathbf{n}_k$ the process and measurement noises, respectively, and $\mathbf{w}_k$ the time-varying system parameters.

Since the parameters $\mathbf{w}$ are unknown and time-varying, the state and parameter must be simultaneously/jointly estimated based on the noisy measured output. On the other hand, the dynamics of the time-varying system parameters are usually hard to describe, i.e., there is a lack of descriptive dynamic equation to characterize the parameters. A commonly used method to address this issue is to treat the parameter as a stochastic signal driven by a white noise ($\mathbf{r}_k$)

$$\mathbf{w}_{k+1} = \mathbf{w}_k + \mathbf{r}_k \tag{2}$$

Then, by concatenating the state and parameter to form an augmented state vector $\mathbf{x}_k^a = \begin{bmatrix}\mathbf{x}_k^T & \mathbf{w}_k^T\end{bmatrix}^T$, joint state space equations (Wan & van der Merwe, 2002) (assuming additive noises) can be obtained as follows

$$\begin{aligned}\begin{bmatrix}\mathbf{x}_{k+1}\\ \mathbf{w}_{k+1}\end{bmatrix} &= \begin{bmatrix}\mathbf{f}\left(\mathbf{x}_k, \mathbf{u}_k, \mathbf{w}_k\right)\\ \mathbf{I}\cdot\mathbf{w}_k\end{bmatrix} + \begin{bmatrix}\mathbf{B}\cdot\mathbf{v}_k\\ \mathbf{r}_k\end{bmatrix} = \mathbf{F}\left(\mathbf{x}_k^a, \mathbf{u}_k\right) + \begin{bmatrix}\mathbf{B}\cdot\mathbf{v}_k\\ \mathbf{r}_k\end{bmatrix}\\ \mathbf{y}_k &= \mathbf{h}\left(\mathbf{x}_k, \mathbf{u}_k, \mathbf{w}_k\right) + \mathbf{n}_k = \mathbf{H}\left(\mathbf{x}_k^a, \mathbf{u}_k\right) + \mathbf{n}_k\end{aligned} \tag{3}$$

The joint estimation problem of states and parameters based on observation can be formulated in an optimal recursive estimation framework as given in the following equation

$$\hat{\mathbf{x}}_k^a = E\left[\mathbf{x}_k^a \middle| \mathbf{Y}_k\right] = E\left[\mathbf{x}_k^a \middle| \mathbf{y}_0, \mathbf{y}_1, \cdots \mathbf{y}_k\right] \tag{4}$$

Two step process (recursively) are involved, the first is the measurement correction

$$p\left(\mathbf{x}_k^a \middle| \mathbf{Y}_k\right) = \frac{p\left(\mathbf{x}_k^a \middle| \mathbf{Y}_{k-1}\right) p\left(\mathbf{y}_k \middle| \mathbf{x}_k^a\right)}{p\left(\mathbf{y}_k \middle| \mathbf{Y}_{k-1}\right)} \tag{5}$$

And the second is the one-step prediction

$$p\left(\mathbf{x}_{k+1}^a \middle| \mathbf{Y}_k\right) = \int p\left(\mathbf{x}_{k+1}^a \middle| \mathbf{x}_k^a\right) p\left(\mathbf{x}_k^a \middle| \mathbf{Y}_k\right) d\mathbf{x}_k^a \tag{6}$$

Various filtering techniques can be implemented in this general recursive estimation framework, including the most widely used extended Kalman filter (EKF), particle filtering (PF), and unscented Kalman filter (UKF). EKF is difficult to tune, and the Jacobian is usually hard to derive, and it can only handle limited amount of nonlinearity, while PF can handle arbitrary distributions and nonlinearities but is computationally very complex. In this paper, we focus on UKF since we believe gives the best tradeoff between PF and EKF.

2.2. UKF Implementation

We assume the additive (zero mean) noise case and follow the UKF procedure given in (Wan & van der Merwe, 2002).

First, the augmented state estimation and covariance matrix are initialized with (7).

$$\begin{aligned}\hat{\mathbf{x}}_0^a &= E\left[\mathbf{x}_0^a\right]\\ \mathbf{P}_0^a &= E\left[\left(\mathbf{x}_0^a - \hat{\mathbf{x}}_0^a\right)\left(\mathbf{x}_0^a - \hat{\mathbf{x}}_0^a\right)^T\right]\end{aligned} \tag{7}$$

Then, for each iteration (k=1,2,…), the sigma points for the state variables in last step are obtained and combined into a matrix as follows

$$\mathbf{X}_{k-1} = \left[\hat{\mathbf{x}}_{k-1}^a \quad \hat{\mathbf{x}}_{k-1}^a + c\sqrt{\mathbf{P}_{k-1}^a} \quad \hat{\mathbf{x}}_{k-1}^a - c\sqrt{\mathbf{P}_{k-1}^a}\right] \tag{8}$$

where $\lambda = \alpha^2\left(L+\kappa\right) - L, c = L + \lambda$, and α, κ and β are all tunable parameters (in this paper, $\alpha = 10^{-3}, \kappa = 0, \beta = 2$ is chosen according to (Wan & van der Merwe, 2002)).

These sigma points are then fed to the state equation to generate a set of new sigma points for the state variables in the current step: $\mathbf{X}_{k|k-1}^{(i)} = \mathbf{F}\left(\mathbf{X}_{k-1}^{(i)}, \mathbf{u}_{\mathbf{k}}\right)$, where the superscript (*i*) denotes the *i*-th column of the corresponding matrix, i.e., the *i*-th sigma point.

The one-step prediction for the augmented state vector in (6) , when implemented with UKF approach, can now be expressed in (9)

$$\begin{aligned}\hat{\mathbf{x}}_k^{a-} &= \sum_{i=0}^{2L} w_i^m \cdot \mathbf{X}_{k|k-1}^{(i)} \\ \mathbf{P}_k^{a-} &= \sum_{i=0}^{2L} w_i^c \cdot \left[\mathbf{X}_{k|k-1}^{(i)} - \hat{\mathbf{x}}_k^{a-}\right]\left[\mathbf{X}_{k|k-1}^{(i)} - \hat{\mathbf{x}}_k^{a-}\right]^T + \mathbf{Q}\end{aligned} \tag{9}$$

where $\mathbf{Q}$ is the process noise covariance matrix, and w_i^m, w_i^c are the weights for the corresponding sigma points.

Measurement correction, on the other hand, is given through (10) – (16)

$$\mathbf{Y}_{k|k-1}^{(i)} = \mathbf{H}\left(\mathbf{X}_{k|k-1}^{(i)}, \mathbf{u}_{\mathbf{k}}\right) \tag{10}$$

$$\hat{\mathbf{y}}_k^- = \sum_{i=0}^{2L} w_i^m \cdot \mathbf{Y}_{k|k-1}^{(i)} \tag{11}$$

$$\mathbf{P}_{\bar{\mathbf{y}}_k\bar{\mathbf{y}}_k} = \sum_{i=0}^{2L} w_i^c \cdot \left[\mathbf{Y}_{k|k-1}^{(i)} - \hat{\mathbf{y}}_k^-\right]\left[\mathbf{Y}_{k|k-1}^{(i)} - \hat{\mathbf{y}}_k^-\right]^T + \mathbf{R} \tag{12}$$

$$\mathbf{P}_{\bar{\mathbf{x}}_k\bar{\mathbf{y}}_k} = \sum_{i=0}^{2L} w_i^c \cdot \left[\mathbf{X}_{k|k-1}^{(i)} - \hat{\mathbf{x}}_k^{a-}\right]\left[\mathbf{Y}_{k|k-1}^{(i)} - \hat{\mathbf{y}}_k^-\right]^T \tag{13}$$

$$\mathbf{K}_k = \mathbf{P}_{\bar{\mathbf{x}}_k\bar{\mathbf{y}}_k}\mathbf{P}_{\bar{\mathbf{y}}_k\bar{\mathbf{y}}_k}^{-1} \tag{14}$$

$$\hat{\mathbf{x}}_k^a = \hat{\mathbf{x}}_k^{a-} + \mathbf{K}_k\left(\mathbf{y}_k - \hat{\mathbf{y}}_k^-\right) \tag{15}$$

$$\mathbf{P}_k^a = \mathbf{P}_k^{a-} - \mathbf{K}_k\mathbf{P}_{\bar{\mathbf{y}}_k\bar{\mathbf{y}}_k}\mathbf{K}_k^T \tag{16}$$

where $\mathbf{R}$ is the measurement noise covariance matrix. The weights typically employed in UKF are given as follows:

$$\begin{aligned} w_0^m &= \lambda/c \\ w_0^m &= \lambda/c + \left(1 - \alpha^2 + \beta\right) \\ w_i^m &= w_i^c = \lambda/2c \end{aligned}$$

2.3. UKF Approach for Prediction

The Bayesian method is an iterative method that involves two steps in each iteration, i.e., prediction and measurement correction. In the general Bayesian estimation framework, the one-step prediction in (6) can be extended to (*m*+1)-step long-term prediction as follows,

$$\begin{aligned} p\left(\mathbf{x}_{\mathbf{k}+m+1}^a \middle| \mathbf{Y}_{\mathbf{k}}\right) &= \int p\left(\mathbf{x}_{\mathbf{k}+m+1}^a \middle| \mathbf{x}_{\mathbf{k}+m}^a\right) p\left(\mathbf{x}_{\mathbf{k}+m}^a \middle| \mathbf{Y}_{\mathbf{k}}\right) d\mathbf{x}_{\mathbf{k}+m}^a \\ &= \int p\left(\mathbf{x}_{\mathbf{k}+m+1}^a \middle| \mathbf{x}_{\mathbf{k}+m}^a\right)\left[\int p\left(\mathbf{x}_{\mathbf{k}+m}^a \middle| \mathbf{x}_{\mathbf{k}+m-1}^a\right) p\left(\mathbf{x}_{\mathbf{k}+m-1}^a \middle| \mathbf{Y}_{\mathbf{k}}\right) d\mathbf{x}_{\mathbf{k}+m-1}^a\right] d\mathbf{x}_{\mathbf{k}+m}^a \\ &= \iint p\left(\mathbf{x}_{\mathbf{k}+m+1}^a \middle| \mathbf{x}_{\mathbf{k}+m}^a\right) p\left(\mathbf{x}_{\mathbf{k}+m}^a \middle| \mathbf{x}_{\mathbf{k}+m-1}^a\right) p\left(\mathbf{x}_{\mathbf{k}+m-1}^a \middle| \mathbf{Y}_{\mathbf{k}}\right) d\mathbf{x}_{\mathbf{k}+m-1}^a d\mathbf{x}_{\mathbf{k}+m}^a \\ &= \int \cdots \int p\left(\mathbf{x}_{\mathbf{k}}^a \middle| \mathbf{Y}_{\mathbf{k}}\right) \prod_{j=k}^{k+m} p\left(\mathbf{x}_{j+1}^a \middle| \mathbf{x}_j^a\right) d\mathbf{x}_{\mathbf{k}}^a \cdots d\mathbf{x}_{\mathbf{k}+m}^a \end{aligned} \tag{17}$$

In this case of (*m*+1)-step long-term prediction, when implemented with UKF approach, the equations (9) can be written as (18),

$$\begin{aligned} \mathbf{X}_{n|n-1}^{(i)} &= \mathbf{F}\left(\mathbf{X}_{k-1}^{(i)}, \mathbf{u}_n\right) \\ \hat{\mathbf{x}}_n^a &= \sum_{i=0}^{2L} w_i^m \cdot \mathbf{X}_{n|n-1}^{(i)} \\ \mathbf{P}_n^a &= \sum_{i=0}^{2L} w_i^c \cdot \left[\mathbf{X}_{n|n-1}^{(i)} - \hat{\mathbf{x}}_n^a\right]\left[\mathbf{X}_{n|n-1}^{(i)} - \hat{\mathbf{x}}_n^a\right]^T + \mathbf{Q} \end{aligned} \tag{18}$$

As can be seen from (18), the long-term prediction utilizes only the one-step prediction iteratively without measurement correction, since the future measurement is unavailable at the current step when prediction is made. Equivalently, the standard UKF procedure can be used with the Kalman gain in (15) set to 0, i.e., $\mathbf{K}_k = \mathbf{0}$.

Also note that in (18), the system input $\mathbf{u}_n$ at step *n* (*n* > *k*) is required to generate the new set of sigma points at each iteration. Generally speaking, the future input can be obtained by analyzing its past stochastic feature and then projecting into the future, while at the same time including the uncertainty of the input itself. For simplicity purpose, in this paper, the current input $\mathbf{u}_k$ is taken as the constant input for all future steps during the prediction, and the uncertainty issue is not considered.

3. AGING MODEL FOR CATALYST DEGRADATION

Aging model is essential to the physics-based prognostic and health monitoring approaches. While extensive researches have been carried out on control and dynamical modeling for fuel cell system, modeling work addressing PEMFC degradation and corresponding health-monitoring and prognostic system has been much less reported. Many of the degradation models have little physical basis, and thus have no predictive capability (A.A. Franco & Tembely, 2007). Franco et al. (A. A. Franco, Schott, Jallut, & Maschke, 2007; Alejandro A. Franco et al., 2009; Alejandro A. Franco & Gerard, 2008) have done a series of leading work on developing a multi-scale mechanistic model of the electrochemical aging processes in a PEMFC to describe, in particular, the carbon corrosion at the cathode, the cathodic oxidation/dissolution of platinum and the carbon supported platinum electrochemical ripening. However, its CFD modeling approach makes it unsuitable for the on-line

prognostic purpose due to the computation burden involved. Also, the model needs too many parameters that are hard to obtain. Darling and Meyers (R.M. Darling & Meyers, 2003) proposed a spatially lumped model that treats a single, porous platinum electrode and the ionomeric solution that fills the pores of the electrode. The model includes spherical platinum particles that can grow and shrink as platinum plates and dissolves; a platinum oxide layer; and an ionic platinum species in solution (Pt^{2+}). The kinetic expressions for platinum oxidation and dissolution developed in this work is incorporated by the same authors (Robert M. Darling & Meyers, 2005) in a transient, one-dimensional mathematical model of the cross section of a PEM fuel cell. In this model, each electrode contains two platinum particle sizes, enabling a description of electrochemically driven transfer of platinum between particles of different sizes. That is, platinum can be exchanged between particles by dissolution and crystallization, capturing the underlying principles of the quasi-Ostwald ripening. Based on their work, we proposed a 64-particle catalyst degradation model (Xian, 2012) and, for the prognostic purpose, simplified the detailed model to a second order aging model. For simplicity of demonstration, in this paper, we further simplify that model to a first order dynamic model, as shown in (19), by neglecting the dynamics of the platinum oxide coverage during the load cycling. The geometric catalytic surface area A_{geo} can then be described as follows

$$\frac{dA_{\text{geo}}}{dt} = -\frac{k_1}{V_{\text{Pt}}^2}\frac{M_{\text{Pt}}}{\rho_{\text{Pt}}}\frac{F\alpha_1}{RT}\beta_r^2 \cdot \exp\left(\frac{F\alpha_1}{RT}\frac{A_{\text{geo}}}{3V_{\text{Pt}}}\right)\cdot A_{\text{geo}}^3 \eta\left(\Delta\phi_c\right) \quad (19)$$

where k_1 is a constant characteristic of the kinetic rate of the reaction, and is usually determined by experiments; V_{Pt} is the total volume of the Pt catalyst; F is the Faraday constant, R is the universal gas constant (J/mol·K) and T the absolute temperature (K); β_r is a system parameter to be identified and represents the relative distribution of the particles radii; $\Delta\phi_c$ is the phase potential difference between the electrolyte phase and the cathode phase, and $\eta(\bullet)$ is a function; M_{Pt} and ρ_{Pt} are the molecular weight and density of platinum, respectively; $\alpha_1 = 1.14\times10^{-10}$.

Since k_1 is extremely small in value, we can scale the above equation in time with a scaling coefficient ε to denote its slowness explicitly. Also note that k_1 is an implicit function of the temperature T, thus we can write the degradation rate of the catalytic surface area as a function of the input potential load, the temperature, the parameter β_r , and the catalytic surface area itself.

$$\frac{dA_{\text{geo}}}{dt} = \varepsilon \cdot \mathbf{g}\left(A_{\text{geo}}, \Delta\phi_c, \beta_r, T\right) \quad (20)$$

Now, by taking into account the uncertain factors as additive process noise, the following stochastic degradation model can be obtained

$$\begin{aligned} \frac{dA_{\text{geo}}}{dt} &= \varepsilon \cdot \mathbf{g}\left(A_{\text{geo}}, \Delta\phi_c, \beta_r, T\right) + w_1(t) \\ \dot{\beta}_r &= w_2(t) \end{aligned} \quad (21)$$

where the unknown time-varying parameter β_r is taken as a state variable, and its derivative as a process noise.

The cell voltage given in (22) is utilized as the measured system output,

$$\begin{aligned} V_{cell} = E_0(T_{\text{fc}}) &- \frac{RT_{\text{fc}}}{4(1-\alpha)F}\ln\left(i+i_{leak}\right) + \frac{RT_{\text{fc}}}{4(1-\alpha)F}\ln\xi_{\text{cat}} \\ &+ \frac{RT_{\text{fc}}}{2F}\ln p_{H_2}^* + \frac{RT_{\text{fc}}}{4(1-\alpha)F}\ln p_{O_2}^* - i\cdot A_{\text{fc}}\cdot R_{ohm} \end{aligned} \quad (22)$$

where $E_0(T_{\text{fc}})$ is the voltage component that only depends on the fuel cell temperature for a specific type of fuel cell; α is the transfer coefficient of the oxygen reduction reaction; i and i_{leak} are the current density and the leak current density; $p_{H_2}^*, p_{O_2}^*$ are the hydrogen and oxygen partial pressures at the reaction site; and R_{ohm} is the total ohmic resistance of the fuel cell. $\xi_{\text{cat}} = \dfrac{A_{\text{geo}}}{A_{\text{geo}}\big|_{t=0}}$ is the ratio of current and initial catalytic geometric (or equivalently electrochemical) surface area, the value of which is 1 when the fuel cell is at its fresh state.

4. APPLICATION OF THE UKF APPROACH FOR DAMAGE TRACKING AND PROGNOSTICS OF PEMFC

The performance degradation of the PEMFC, characterized by the voltage drop under the same level of current load, typically goes through two stages. In the first stage, the PEMFC experiences a gradual performance loss caused by the slowly decreasing ECSA that can be described by the degradation model (21) presented in the last section; in contrast, the second stage is characterized by a much more abrupt performance drop that leads to the total loss of the power output capability of the PEMFC, resulting from the mechanical breach (pinholes) formed in the polymer membrane. As it may seem obvious that the second stage, if detected, can be utilized to determine the end-of-life of the PEMFC, the gradual loss of the ECSA in the first stage can also lead to serious performance loss to the extent that failure of the system can be declared. In (Shimoi, Aoyama, & Iiyama, 2009) , actual vehicle tests are carried out to collect the PEMFC stack durability data until the performance is deemed low. The post-test analysis of the

membrane-electrolyte-assembly (MEA) reveals no crack is developed in the membrane and suggests that the voltage drop is mainly attributed to the reduced ECSA at the cathode of the fuel cells. Therefore in this paper, as a first step, we only investigate the health monitoring and prognostic problem for the catalyst degradation.

4.1. Data Preprocessing

From (22), it is obvious that the measured voltage ("feature") is not only a function of the slowly varying damage variables, i.e, i_{leak} and ξ_{cat}, but also a function of the fast varying system variables $p^*_{H_2}, p^*_{O_2}$. To obtain an output variable that is solely related to the slowly varying damage variables, i.e., the state variables in the aging model describing the degradation process, we propose the following data preprocessing system, as shown in Figure 1.

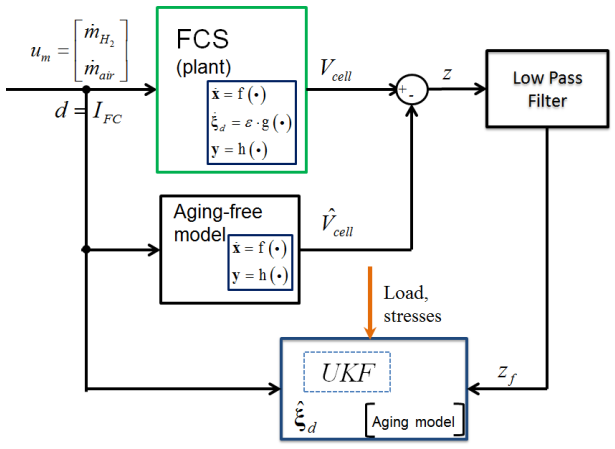

Figure 1 Preprocessing of the output signal for UKF

Basically, the method above utilizes an aging-free dynamic model of the fuel cell system that captures the fast dynamics of the FCS in the normal time scale while assuming constant, non-degrading damage variables in the long time scale. The model output is given in (23).

$$\hat{V}_{cell} = E_0\left(T_{\text{fc}}\right) + \frac{RT_{\text{fc}}}{2F}\ln \hat{p}^*_{H_2} + \frac{RT_{\text{fc}}}{4(1-\alpha)F}\ln \hat{p}^*_{O_2} - i\cdot A_{\text{fc}}\cdot R_{ohm} - \frac{RT_{\text{fc}}}{4(1-\alpha)F}\ln\left(i + i^0_{leak}\right) \tag{23}$$

where i^0_{leak} is the membrane leak current density at the initial time, and here we assume that the total ohmic resistance R_{ohm} is readily available.

The difference of the outputs of the actual FCS and the aging-free dynamic FCS model can then be calculated and written as follows.

$$V_{cell} - \hat{V}_{cell} = \frac{RT_{\text{fc}}}{4(1-\alpha)F}\ln \xi_{\text{cat}} - \frac{RT_{\text{fc}}}{4(1-\alpha)F}\ln\left(\frac{i + i_{\text{leak}}}{i + i^0_{leak}}\right) + \left(\frac{RT_{\text{fc}}}{2F}\ln\frac{p^*_{H_2}}{\hat{p}^*_{H_2}}\right) + \left[\frac{RT_{\text{fc}}}{4(1-\alpha)F}\ln\frac{p^*_{O_2}}{\hat{p}^*_{O_2}}\right] \tag{24}$$

Ideally, given that the model is accurate in capturing the fast dynamics of the system and no disturbance is present, we have $\frac{p^*_{H_2}}{\hat{p}^*_{H_2}} = 1, \frac{p^*_{O_2}}{\hat{p}^*_{O_2}} = 1$, and the difference in (24) would depend only on the slowly varying damage variables. However, in practice, the instantaneous voltage degradation ($V_{cell} - \hat{V}_{cell}$) would inevitably be affected by modeling error that may result in model prediction deviation especially in transition, and by disturbances such as the water content in the gas diffusion media that could even result in offset between the two outputs at their steady states. By denoting the two kinds of sources of mismatches with n_d and n_s respectively, the difference z in Figure 1 can be expressed as follows,

$$z = \frac{RT_{\text{fc}}}{4(1-\alpha)F}\ln \xi_{\text{cat}} - \frac{RT_{\text{fc}}}{4(1-\alpha)F}\ln\left(\frac{i + i_{\text{leak}}}{i + i^0_{leak}}\right) + n_d + n_s \tag{25}$$

The deviation between the model and the actual plant outputs is then fed to the low pass filter in Figure 1 to remove the fast dynamics mismatch n_d and to obtain the filtered deviation z_f as in (26).

$$z_f = \frac{RT_{\text{fc}}}{4(1-\alpha)F}\ln \xi_{\text{cat}} - \frac{RT_{\text{fc}}}{4(1-\alpha)F}\ln\left(\frac{i + i_{\text{leak}}}{i + i^0_{leak}}\right) + n_s \tag{26}$$

To apply the UKF approach introduced in the previous section, we need to first discretize the continuous system equations. By denoting the fixed sample time as ΔT, the state equations can be written as

$$\begin{aligned} A_{\text{geo},k+1} &= \varepsilon\cdot N_\varepsilon\cdot\Delta T\cdot\left[\mathbf{g}\left(A_{\text{geo},k}, \Delta\phi_{c,k}, \beta_{r,k}, T_{\text{fc}}\right) + w_{1,k}\right] \\ \beta_{r,k+1} &= \beta_{r,k} + \varepsilon\cdot N_\varepsilon\cdot\Delta T\cdot w_{2,k} \end{aligned} \tag{27}$$

and the output equation is given by (28)

$$z_{f,k} = \frac{RT_{\text{fc}}}{4(1-\alpha)F}\ln \xi_{\text{cat},k} - \frac{RT_{\text{fc}}}{4(1-\alpha)F}\ln\left(\frac{i_k + i_{\text{leak},k}}{i_k + i^0_{leak,k}}\right) + n_{s,k} \tag{28}$$

where the k represents the discretization time step. Note that, since the fuel cell catalyst degradation is an extremely slow process (the fresh to failure life cycle typically takes several hundred hours or longer), the sample time ΔT for the discretized model employed by the UKF can be chosen in the hour scale, instead of second, to lower the unnecessary computational burden. In this paper, we choose $\Delta T = 1500s$ (25 min). Under such a slow time scale, disturbances

induced offset between the two voltage outputs $n_{s,k}$ can then be treated reasonably as a white noise.

As seen in Figure 1, $z_{f,k}$ in (28) can be practically obtained as

$$z_{f,k} = \mathrm{LPF}\left(V_{\mathrm{cell},k} - \hat{V}_{\mathrm{cell},k}\right) \tag{29}$$

where LPF stands for the low pass filter.

Simulation is carried out where we assume a cyclic load profile as given in Figure 2.

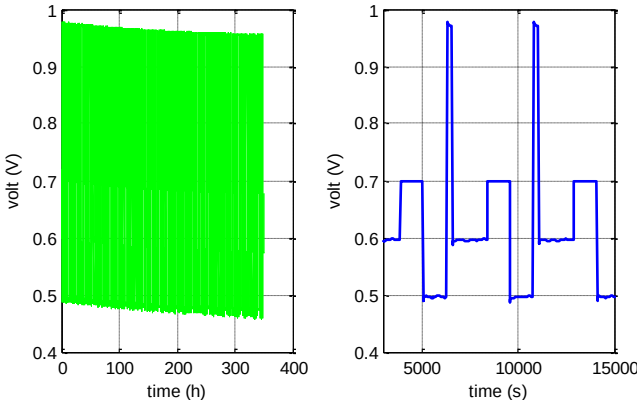

Figure 2 Load profile for PHM scheme simulation validation

4.2. Simulation Results

The simulation result for health monitoring validation is presented in Figure 3. It can be seen that the ECSA has been tracked satisfactorily, while β_r varies between the range [0.03, 0.04], and gradually settles down after 100 hours. In fact, the first 100 hours can be considered as the necessary phase for parameter identification. After this phase, the parameter β_r would stay relatively stable around some constant value. This characteristic feature can also be exploited to perform fault diagnostics for the purpose of early detection of the massive gas crossover.

The parameters used for this simulation are grouped in the following table:

Initial state estimate	$\begin{bmatrix} \hat{A}_{Pt}^0 \\ \hat{\beta}_r^0 \end{bmatrix} = \begin{bmatrix} A_{Pt}^0 \times 1.1 \\ 0.035 \end{bmatrix}$
Initial covariance matrix	$P_0 = \begin{bmatrix} (0.02 \times A_{Pt}^0)^2 & 0 \\ 0 & (0.04 \times 0.15)^2 \end{bmatrix}$
Process noise	$\begin{bmatrix} Q_1 & 0 \\ 0 & Q_2 \end{bmatrix} = diag\left(\begin{bmatrix} (A_{Pt}^0 \times 1 \times 10^{-6})^2 \\ (0.035 \times 2 \times 10^{-6})^2 \end{bmatrix}\right)$
Measurement noise	$R = 6.7 \times 10^{-6}$

Table 1 Parameters used in the simulation

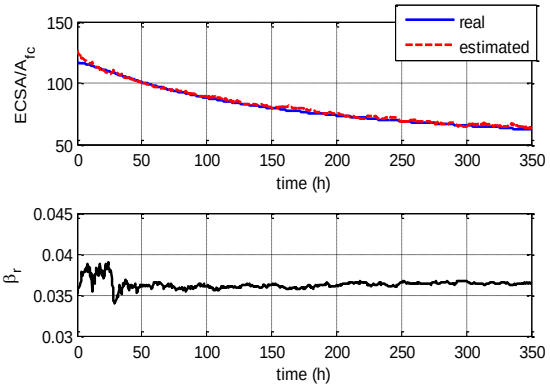

Figure 3 Simulation result for health monitoring

The simulation results for prognostics (long-term prediction of the damage variable) are presented in Figure 4 and Figure 5, at two different prediction time points respectively. For the purpose of demonstration, and without loss of generosity, the threshold for the catalyst failure is set to 63.

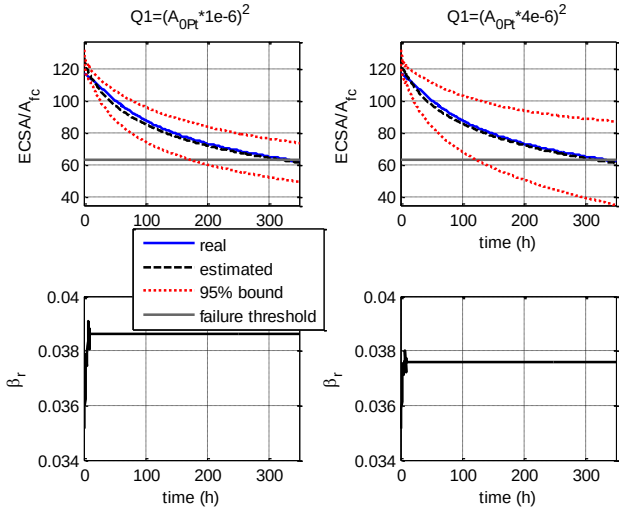

Figure 4 Simulation result for prognostics at the beginning of life (10 hours)

In Figure 4, prognostic is performed at the beginning of life of the fuel cell (10 hours). It can be seen that the 95% error is growing larger with increasing prediction step due to lack

of measurement correction. β_r is seen to be constant all the time with the same reason. Two values for the process noise Q_1 are compared, i.e., $(A_{Pt}^0 \times 1\times 10^{-6})^2$ and $(A_{Pt}^0 \times 4\times 10^{-6})^2$. As expected, the smaller value of the process noise results in narrower 95% bounds, and thus a more accurate prediction.

Figure 5 shows the simulation results with prognostic starting from the middle of the durability test, here at 100 hours. Due to lack of measurement correction, β_r stops updating and is taken as a constant after100 hours. The 95% error is also seen growing larger with increasing prediction step, but much narrower compared to that in Figure 4.

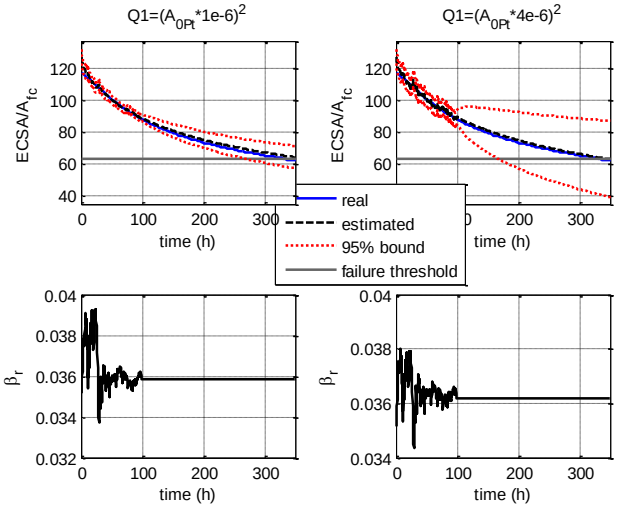

Figure 5 Simulation result for Prognostics at 100h

4.3. Performance Evaluation

To apply any prognostics metrics (Saxena et al., 2008; Saxena, Celaya, Saha, Saha, & Goebel, 2009) for the performance evaluation of the proposed algorithm, it is necessary to first obtain the remaining useful life (RUL) prediction w.r.t. the prediction time t_{pred} based on the information contained in the long-term prediction of the damage variable. By denoting the threshold for the normalized catalytic area to be ξ_{th}, and the RUL (stochastic variable at t_{pred}) to be T_{RUL}, we can establish the following connection between the probability functions of the damage variable and the RUL

$$P\left(\frac{ECSA}{A_{fc}} < \xi_{th} \middle| t\right)\Big|_{t_{pred}} = P\left(\text{fail}\middle| t\right) = P\left(T_{RUL} \le t\right)\Big|_{t_{pred}} = F_{RUL}\left(t\right)\Big|_{t_{pred}} \tag{30}$$

where $t > t_{pred}$ is any future time, $F_{RUL}(t)$ is the cumulative probability function of the RUL, with which the RUL probability density function can be derived as

$$f_{RUL}(t) = \frac{\partial F_{RUL}(t)}{\partial t} \tag{31}$$

Here we employ a metrics called α performance, which is similar to the $\alpha - \lambda$ performance proposed in (Saxena et al., 2008) except that the time window is not modified along the prediction time axis. The α performance basically evaluates the probability of the RUL T_{RUL} falling in the time window $\left[(1-\alpha)t_{EOL} \quad (1+\alpha)t_{EOL}\right]$ defined by the parameter α. The probability can be calculated as follows

$$\begin{aligned} P_\alpha &= \int_{(1-\alpha)t_{EOL}}^{(1+\alpha)t_{EOL}} f_{RUL}(t)\,dt \\ &= F_{RUL}\left[(1+\alpha)t_{EOL}\right] - F_{RUL}\left[(1-\alpha)t_{EOL}\right] \end{aligned} \tag{32}$$

Figure 6 presents the RUL prediction at selected prediction time, with the following process noise (other simulation parameters are the same as that in Table 1) assumed for the dynamic aging process. α is chosen to be 15% in this case.

$$\begin{bmatrix} Q_1 & 0 \\ 0 & Q_2 \end{bmatrix} = diag\left(\begin{bmatrix} (A_{Pt}^0 \times 8\times 10^{-7})^2 \\ (0.035\times 1\times 10^{-6})^2 \end{bmatrix}\right)$$

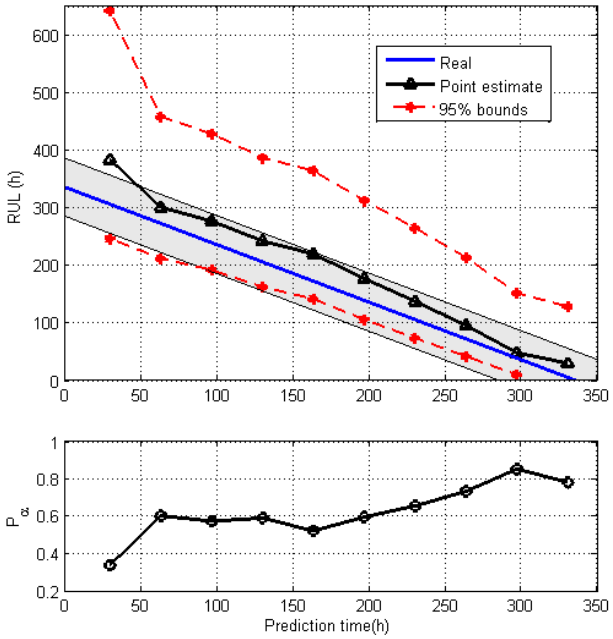

Figure 6 RUL prediction plot (α = 15%)

As can be seen from Figure 6, the point estimate of the RUL is contained in the time window (the shaded area in the figure) for the majority of the prognostic process. The

prognostic process is a dynamic process in that the RUL prediction is updated dynamically as the prediction time proceeds. It can also be seen that, with a constant α time window, the probability P_α shows an increasing trend along with the prognostic process, indicating improved accuracy of the prediction.

It is noted that α performance can also be considered as a variant of prognostic horizon (PH) metrics (Saxena et al., 2008) and can be readily converted to it if necessary.

5. CONCLUSION

Prognostics problem of the PEMFC is studied in this paper. A prognostic-oriented aging model is presented to describe the slowly-varying dynamics in the fuel cell that characterize the degradation process of the catalyst of the fuel cell. An UKF-based framework is proposed for the health monitoring and prognostic scheme and applied to solve the problems. The outcome of the prognosis scheme provides information about the precision and accuracy of long-term prediction, RUL expectations and 95% confidence intervals. Simulation is carried out for the validation of the proposed scheme with relevant prognostics metrics. The results show that with measurement correction, the health monitoring system can successfully track the damage variable throughout the degradation process; while at any time during the aging process, the remaining useful life can be predicted with satisfactory accuracy given that future load input information is precisely known.

REFERENCES

Daigle, M., Saha, B., & Goebel, K. (2012). A comparison of filter-based approaches for model-based prognostics. *2012 IEEE Aerospace Conference* (pp. 1 –10). Presented at the 2012 IEEE Aerospace Conference. doi:10.1109/AERO.2012.6187363

Darling, R.M., & Meyers, J. P. (2003). Kinetic model of platinum dissolution in PEMFCs. *Journal of the Electrochemical Society*, J. Electrochem. Soc. (USA), *150*(11), 1523–7. doi:10.1149/1.1613669

Darling, Robert M., & Meyers, J. P. (2005). Mathematical model of platinum movement in PEM fuel cells. *Journal of the Electrochemical Society*, *152*(1), A242–A247. doi:10.1149/1.1836156

Franco, A. A., Schott, P., Jallut, C., & Maschke, B. (2007). A Multi-Scale Dynamic Mechanistic Model for the Transient Analysis of PEFCs. *Fuel Cells*, *7*(2), 99–117. doi:10.1002/fuce.200500204

Franco, A.A., & Tembely, M. (2007). Transient multiscale modeling of aging mechanisms in a PEFC cathode. *Journal of the Electrochemical Society*, *154*, B712.

Franco, Alejandro A., Coulon, R., Ferreira de Morais, R., Cheah, S. K., Kachmar, A., & Gabriel, M. A. (2009). Multi-scale Modeling-based Prediction of PEM Fuel Cells MEA Durability under Automotive Operating Conditions (pp. 65–79). ECS. doi:10.1149/1.3210560

Franco, Alejandro A., & Gerard, M. (2008). Multiscale Model of Carbon Corrosion in a PEFC: Coupling with Electrocatalysis and Impact on Performance Degradation. *Journal of The Electrochemical Society*, *155*(4), B367. doi:10.1149/1.2838165

Franco, Alejandro A., Gerard, M., Guinard, M., Barthe, B., & Lemaire, O. (2008). Carbon Catalyst-Support Corrosion in Polymer Electrolyte Fuel Cells: Mechanistic Insights (pp. 35–55). ECS. doi:10.1149/1.3002807

Okada, T. (2003). Effect of Ionic contaminants. *Handbook of Fuel Cells – Fundamentals, Technology and Applications* (pp. 627–646). Wiley & Sons.

Orchard, M. E, & Vachtsevanos, G. J. (2009). A particle-filtering approach for on-line fault diagnosis and failure prognosis. *Transactions of the Institute of Measurement and Control*, *31*(3-4), 221–246.

Orchard, M., Wu, B., & Vachtsevanos, G. (2005). A particle filtering framework for failure prognosis. *2005 World Tribology Congress III, September 12, 2005 - September 16, 2005*, Proceedings of the World Tribology Congress III - 2005 (pp. 883–884). Washington, D.C., United states: American Society of Mechanical Engineers.

Orchard, Marcos E., & Vachtsevanos, G. J. (2007). A particle filtering-based framework for real-time fault diagnosis and failure prognosis in a turbine engine. *2007 Mediterranean Conference on Control and Automation, MED, July 27, 2007 - July 29, 2007*, 2007 Mediterranean Conference on Control and Automation, MED. Athens, Greece: Inst. of Elec. and Elec. Eng. Computer Society. doi:10.1109/MED.2007.4433871

Saha, B., & Goebel, K. (2008). Uncertainty management for diagnostics and prognostics of batteries using Bayesian techniques. *Aerospace Conference, 2008 IEEE* (pp. 1–8).

Saha, B., Goebel, K., Poll, S., & Christophersen, J. (2007). An integrated approach to battery health monitoring using bayesian regression and state estimation. *Autotestcon, 2007 IEEE* (pp. 646–653).

Saha, B., Goebel, K., Poll, S., & Christophersen, J. (2009). Prognostics Methods for Battery Health Monitoring Using a Bayesian Framework. *IEEE Transactions on Instrumentation and Measurement*, *58*(2), 291–296. doi:10.1109/TIM.2008.2005965

Saxena, A., Celaya, J., Balaban, E., Goebel, K., Saha, B., Saha, S., & Schwabacher, M. (2008). Metrics for evaluating performance of prognostic techniques. *Prognostics and Health Management, 2008. PHM 2008. International Conference on* (pp. 1–17).

Saxena, A., Celaya, J., Saha, B., Saha, S., & Goebel, K. (2009). On applying the prognostic performance metrics. *Proceedings of the annual conference of the prognostics and health management society*. Retrieved

from http://72.27.231.73/sites/phmsociety.org/files/phm_submission/2009/phmc_09_39.pdf

Schmittinger, W., & Vahidi, A. (2008). A review of the main parameters influencing long-term performance and durability of PEM fuel cells. *Journal of Power Sources*, J. Power Sources (Switzerland), *180*(1), 1–14. doi:10.1016/j.jpowsour.2008.01.070

Shimoi, R., Aoyama, T., & Iiyama, A. (2009). *Development of Fuel Cell Stack Durability based on Actual Vehicle Test Data: Current Status and Future Work* (No. 2009-01-1014). Warrendale, PA: SAE International. Retrieved from http://www.sae.org/technical/papers/2009-01-1014

Wan, E. A., & van der Merwe, R. (2002). The Unscented Kalman Filter. In S. Haykin (Ed.), *Kalman Filtering and Neural Networks* (pp. 221–280). John Wiley & Sons, Inc. Retrieved from http://onlinelibrary.wiley.com/doi/10.1002/0471221546.ch7/summary

Xian, Z. (2012). *Prognostic and Health-Management Oriented Fuel Cell Modeling and On-line Supervisory System Development*. Clemson University.

BIOGRAPHIES

Xian Zhang received his B.S. and M.S. degrees in Automotive Engineering from Tsinghua University, Beijing, China, in 2005 and 2007, respectively, and just received his Ph.D. degree in Automotive Engineering from Clemson University, Clemson, SC in August 2012. His Ph.D. research area was in the control, diagnostics and prognostics of the PEMFC system. From September 2007 to May 2012, he was a Graduate Research Assistant with the International Center for Automotive Research and Department of Automotive Engineering, Clemson University. From June to November 2010, he was an intern with National Transportation Research Center (NTRC), at Oak Ridge National Lab. Xian Zhang is a student member of ASME and SAE.

Pierluigi Pisu is an Assistant Professor at the Department of Automotive Engineering and holds a joint appointment with the Department of Electrical and Computer Engineering at Clemson University. He received his Ph.D. in Electrical Engineering from the Ohio State University in 2002. In 2004, Dr. Pisu was granted two US patents in area of model-based fault detection and isolation. Dr. Pisu's research interests are in the area of fault diagnosis and prognosis with application to vehicle systems, energy management control of hybrid electric vehicles, vehicle to grid interaction, and systems aging. He also worked in the area of sliding mode and robust control. Dr. Pisu is member of IEEE, ASME and SAE. He is member of the IEEE Technical Committee in Automotive Control, IFAC Technical Committee in Automotive Control, Associate Editor of the Conference Editorial Board of the IEEE Control Systems Society, and Associate Editor of the SAE Journal on Alternative Powertrains.